Recent peat and carbon accumulation following the Little Ice Age in northwestern Quebec, Canada

Piilo, Sanna

2019-07

Piilo , S , Zhang , H , Garneau , M , Gallego-Sala , A V , Amesbury , M & Väliranta , M 2019 , ' Recent peat and carbon accumulation following the Little Ice Age in northwestern Quebec, Canada ' , Environmental Research Letters , vol. 14 , no. 7 , 075002 . https://doi.org/10.1088/1748-9326/ab11ec

http://hdl.handle.net/10138/304557
https://doi.org/10.1088/1748-9326/ab11ec

Recent peat and carbon accumulation following the Little Ice Age in northwestern Québec, Canada

Environmental Research Letters

LETTER

Recent peat and carbon accumulation following the Little Ice Age in northwestern Québec, Canada

Sanna R Piilo[1,2], **Hui Zhang**[1,2], **Michelle Garneau**[3], **Angela Gallego-Sala**[4], **Matthew J Amesbury**[1,4] and **Minna M Väliranta**[1,2]

[1] ECRU, Ecosystems and Environment Research Programme, Department of Environmental Sciences, University of Helsinki, PO Box 65, FI-00014, Finland
[2] Helsinki Institute of Sustainability Science (HELSUS), Finland
[3] Department of Geography, Université du Québec à Montréal, Canada
[4] Geography, College of Life and Environmental Sciences, University of Exeter, United Kingdom

E-mail: sanna.piilo@helsinki.fi

OPEN ACCESS

RECEIVED
23 October 2018

REVISED
17 March 2019

ACCEPTED FOR PUBLICATION
21 March 2019

PUBLISHED
26 June 2019

Keywords: permafrost peatlands, climate warming, vegetation dynamics, carbon accumulation, plant macrofossil analysis

Supplementary material for this article is available online

Abstract

Peatland ecosystems are important carbon sinks, but also release carbon back to the atmosphere as carbon dioxide and methane. Peatlands therefore play an essential role in the global carbon cycle. However, the response of high-latitude peatlands to ongoing climate change is still not fully understood. In this study, we used plant macrofossils and peat property analyses as proxies to document changes in vegetation and peat and carbon accumulation after the Little Ice Age. Results from 12 peat monoliths collected in high-boreal and low-subarctic regions in northwestern Québec, Canada, suggest high carbon accumulation rates for the recent past (post AD 1970s). Successional changes in plant assemblages were asynchronous within the cores in the southernmost region, but more consistent in the northern region. Average apparent recent carbon accumulation rates varied between 50.7 and 149.1 g C m^{-2} yr^{-1} with the northernmost study region showing higher values. The variation in vegetation records and peat properties found within samples taken from the same sites and amongst cores taken from different regions highlights the need to investigate multiple records from each peatland, but also from different peatlands within one region.

Introduction

Future changes in climate can be expected to influence peatland vegetation and related carbon dynamics, especially in the high-latitudes where warming is most pronounced, almost twice the global average (IPCC 2013). Permafrost peatlands are especially sensitive to climate change, namely changes in temperatures and moisture balance (precipitation minus evaporation) which determine vegetation and carbon cycling processes (Ovenden 1990, Carroll and Crill 1997, Davidson and Janssens 2006, Swindles *et al* 2015, Gałka *et al* 2017, 2018). Despite covering only ca. 5% of Earth's landmass (Yu *et al* 2010), peatlands form a major terrestrial carbon sink (Gorham 1991, Yu *et al* 2009, 2010) and are connected to the global carbon cycle and its associated carbon-climate feedbacks (Frolking and Roulet 2007, McGuire *et al* 2009, Yu 2011). However, there are still large uncertainties about future climate-induced changes in peatland dynamics driven by changes in vegetation assemblages and moisture conditions (McGuire *et al* 2018).

Due to climate warming, net primary productivity (NPP) will likely increase because of longer growing seasons (Gallego-Sala *et al* 2018). This could accelerate peat accumulation, an effect that may be partly, or even wholly, mitigated by an increase in peat decomposition (Ise *et al* 2008, Dorrepaal *et al* 2009, Crowther *et al* 2016). Yu *et al* (2009) and Charman *et al* (2013) have shown that during past warm periods increases in NPP exceeded increases in peat decomposition, leading to higher rates of peat accumulation. The overall predicted 30% increase in precipitation (Collins *et al* 2013) may also enhance peat accumulation if not

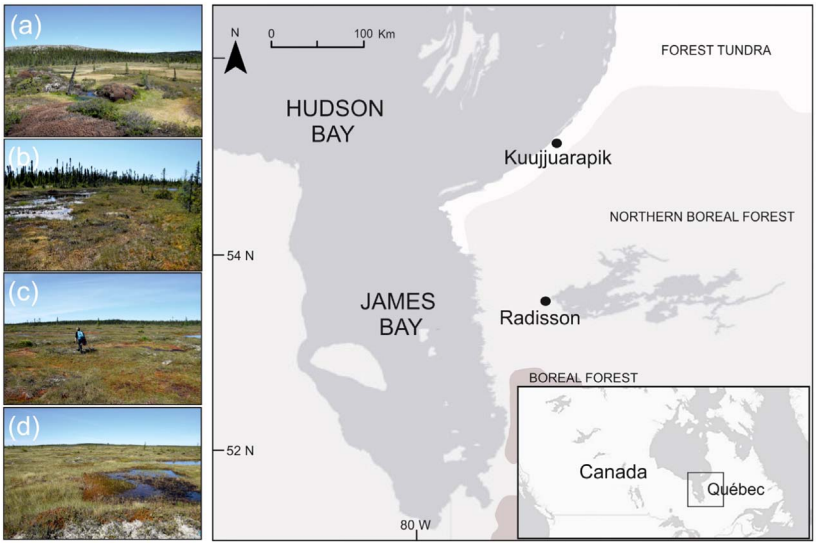

Figure 1. Study site locations marked with dots (Kuujjuarapik and Radisson). Pictures from the coring sites, (a): K1P, (b): K2, (c): Rad, and (d): LG2. Basemap: Esri, HERE, Garmin © OpenStreetMap contributors. CC BY-SA.

reversed by increase in evapotranspiration (Yu *et al* 2009).

In the James Bay and Hudson Bay Lowlands, peatlands cover vast areas and have stored ca. 30 Pg carbon since their initiation during the mid-Holocene (Packalen *et al* 2014). Many previous studies have investigated Holocene carbon dynamics in eastern Canada (e.g. Charman *et al* 1994, van Bellen *et al* 2011a, 2011b, Garneau *et al* 2014, Packalen and Finkelstein 2014, Magnan and Garneau 2014a, 2014b, Charman *et al* 2015) showing high regional variability in both apparent rates of carbon accumulation and in the timing of shifts in carbon accumulation throughout the Holocene. Studies focusing on more recent carbon dynamics and response to ongoing rapid climate change in northwestern Québec are sparse (see, however, Ali *et al* 2008, Beaulieu-Audy *et al* 2009, Loisel and Garneau 2010, Lamarre *et al* 2012).

To address the knowledge gap on the developmental and carbon dynamics of high-latitude peatlands after the Little Ice Age (LIA) (anno Domini (AD) 1450–1850 (Naulier *et al* 2015, Wilson *et al* 2016)), we examined several peat sections collected from two ecoregions (high-boreal and low-subarctic), in northwestern Québec. Climate started to warm after the LIA and since the 1970s human-induced warming has been more prominent (PAGES 2k Consortium 2013, Abram *et al* 2016). Increased snowfall since the 1950s and warm temperatures in the 1990s triggered rapid permafrost melting on the eastern coast of Hudson Bay (Payette *et al* 2004). Hence, permafrost is predicted to disappear from subarctic Québec in the coming decades (Payette *et al* 2004, Jean and Payette 2014), likely altering the vegetation and thus peatland carbon dynamics of the region (Swindles *et al* 2015).

This study investigates the response of northern peatland vegetation and carbon accumulation dynamics to recent warming in northwestern Québec. Plant macrofossil analysis was used as a primary proxy to reconstruct past habitat changes (see Väliranta *et al* 2007, 2017). ^{14}C and ^{210}Pb chronologies in combination with peat property analyses enabled the reconstruction of peat and carbon accumulation. Replicate records from each peatland and from proximal locations inside the study regions allowed us to estimate if detected changes were climate-induced or driven by internal dynamics (Swindles *et al* 2012, Mathijssen *et al* 2016, 2017, Magnan *et al* 2018). Specifically we evaluated: (1) if plant assemblages are changing synchronously in response to rapid recent warming, (2) if warmer climate has increased peat plant NPP and thus carbon accumulation rates, especially in the southern range of the study region, and (3) if multiple cores provide better assessment of within and between site variability.

Methods

Study sites

We selected two regions in northwestern Québec: one within the sporadic and the other within the discontinuous permafrost zone (Allard and K-Seguin 1987, Thibault and Payette 2009). Kuujjuarapik (K1P and K2) represents the subarctic, forested tundra ecoregion at the southernmost limit of the discontinuous permafrost zone (figure 1). Palsa mounds are characteristic at K1P peatland, whereas K2 is a small fen with peat thickness of 1–2 m. Radisson (LG2 and Rad) represents the northernmost boreal ecoregion (figure 1). These two peatlands, in region of sporadic permafrost, are ombrotrophic with peat thickness of 3−4 m (Thibault and Payette 2009).

In the two study regions, mean annual temperatures are below 0 °C (table 1). Mean annual temperatures have increased in both regions (table 1). In

Table 1. Study site information. Meteorological data for 30 year (1981–2010) measuring period: mean annual temperature (MAT), mean annual precipitation (MAP), and growing degree-days above zero (GDD0), measured from stations; La Grande Riviere A in Radisson and Kuujjuarapik station A (Environment Canada 2018). Increases in MAT, MAP, and GDD0 since 1961 and/or 1971 until present. Meters above sea level (MASL). Dominant vegetation around the coring points listed.

Location	MAT (°C)	MAP (mm)	GDD0	Core name	Latitude (N)	Longitude (W)	MASL (m)	Dominant vegetation
Kuujjuarapik				K1P1	55 °13′35.8″	77 °41′41.2″	100	*Sphagnum fuscum, S. capillifolium, Cladonia spp., Chamaedaphne calyculata, Kalmia polifolia, Rhododendron groenlandicum Andromeda polifolia, Vaccinium uliginosum, V. oxycoccos, Trichophorum cespitosum, Carex* spp., *Rubus chamaemorus, Drosera rotundifolia*
1981–2010	−4.0	661	1384	K1P2	55 °13′34.9″	77 °41′47.8″		
Increase since				K1P3	55 °13′34.0″	77 °41′54.7″		
1961until present	0.5	46		K2.1	55 °13′38.6″	77 °42′18.4″	115	
1971 until present	0.4	12	74	K2.2	55 °13′38.2″	77 °42′19.5″		
				K2.3	55 °13′38.2″	77 °42′20.6″		
Radisson				LG2.1	53 °39′09.4″	77 °44′00.2″	175	
1981–2010	−2.9	697	1684	LG2.2	53 °39′08.6″	77 °43′56.2″		
Increase since				LG2.3	53 °39′04.1″	77 °43′50.3″		
1971 until present	0.2	13	62	Rad1	53 °39′38.6″	77 °44′51.9″	170	
				Rad2	53 °39′42.0″	77 °44′52.9″		
				Rad3	53 °39′45.1″	77 °44′52.7″		

Table 2. Core length (cm) represents the thickness of the unfrozen peat layer at the time of the sampling. Water table depth (WTD). Average peat accumulation rates (peat accu.) mm yr^{-1}. Average recent apparent carbon accumulation rates (RERCA) (g C m^{-2} yr^{-1}) were calculated for periods AD 1850, AD 1900, and AD 1950 until present. NA: not available indicates that the chronology does not reach that far back in time. Basal ages from the core bottoms (cal. BP) are rounded to nearest five.

Core	Core length (cm)	WTD (cm)	Peat accu. (mm yr^{-1})	Basal age of the core Cal. BP	RERCA AD1950	RERCA AD1900	RERCA AD1850
K1P1	39	13	1.7	340	70.1	60.1	53.0
K1P2	35	18	1.6	2530	91.7	82.6	74.3
K1P3	31	18	3.2	185	121.0	108.4	101.8
K2.1	32	27	3.5	140	102.1	89.3	83.3
K2.2	31	22	4.9	50	149.1	140.6	NA
K2.3	33	20	5.4	−10	147.9	NA	NA
LG2.1	34	20	2.3	115	65.3	64.6	63.1
LG2.2	33	21	5.4	−10	136.9	NA	NA
LG2.3	34	18	3.2	120	91.9	77.7	71.1
Rad1	38	23	3.2	120	103.3	95.7	89.6
Rad2	37	14	2.9	190	100.0	89.4	81.9
Rad3	36	19	1.7	180	50.7	51.0	54.1

Kuujjuarapik mean summer temperature has increased 1.0 °C since 1961, while mean winter temperature has increased 0.5 °C since 1971 (Environment Canada 2018). In Radisson, since 1971, the biggest seasonal increase of 0.5 °C is in mean autumn temperatures. In Kuujjuarapik, the increase in growing degree-days (GDD0) (between 1971–2000 and 1981–2010) is ca. 6% and in Radisson ca. 4% (table 1). In both regions, autumn rainfall especially has increased. 35%–40% of the precipitation falls as snow.

In the James Bay lowlands, peatlands cover ca. 20%–30% of the land area (Arseneault and Sirois 2004). In Radisson, peat started to accumulate following post glacial land uplift after 8000 calibrated (cal.) yr. before present (BP) (Dyke and Prest 1987, Beaulieu-Audy *et al* 2009). Radisson study sites are characterised by hummock-hollow microforms with e.g. *Sphagnum lindbergii* and *Warnstorfia exannulata* group abundantly present in low lawns and hollows and *S. fuscum* on hummocks while *Picea mariana* is sparsely present (table 1). Along the Hudson Bay lowlands, at the K1P, peat started to accumulate over marine sediments around 5950–5100 cal. BP and palsa formation is connected to the LIA cooling (Arlen-Pouliot and Bhiry 2005; Lamarre *et al* 2012). Ombrotrophic habitat conditions prevail in the central palsa mound part and hummock vegetation in K1P and K2 is largely similar to Radisson peatlands (table 1) but supplemented by e.g. *Polytrichum strictum,* and *Sphagnum russowii*. Sedges dominate the fen habitats together with *Myrica gale, Menyanthes trifoliata, Eriophorum russeolum, S. papillosum, S. riparium,* and brown mosses such as *Scorpidium scorpioides. Larix laricina* is occasionally present.

Sampling

In early July 2017, twelve peat monoliths: three from each four peatlands, K1P, K2, LG2, and Rad, were collected (table 1, figure 1). The core-lengths varied between 32 and 39 cm (table 2). Peat sections (10 cm in diameter) were sampled by hand sawing the layer overlying seasonal frost or permafrost from intermediate lawn microforms (water tables from 13 to 23 cm) inhabited mainly by *Sphagnum fuscum*. Such microhabitats are considered the most sensitive to reflect climate-induced changes in hydrology and consequent plant community shifts (e.g. Väliranta *et al* 2007, Frolking *et al* 2014). The cores were collected from relatively central parts of the peatlands, some tens of meters apart from each other. Peat monoliths were wrapped in plastic film and aluminium foil, transported and frozen at the University of Helsinki, Finland. For the analyses, monoliths were cut into 1 cm slices. To avoid contamination the outmost ca. two centimetres of peat was removed. The subsamples were stored in a cold room at 6 °C in plastic bags.

Plant macrofossil analysis

Plant macrofossil analysis was performed at 2 cm resolution. Where prominent changes in plant composition occurred, the resolution was increased to contiguous centimetres. Volumetric samples of 5 cm^3 were carefully rinsed under running water using a 140 μm sieve. From the residue, proportions of the main peat components (such as *Sphagnum*, non-*Sphagnum* mosses, Cyperaceae remains, wood, roots, and leaves) were estimated as percentages of a total sample volume under a stereomicroscope and a high-power light microscope. Seeds, leaves and charred remains were counted as exact numbers. Plant macrofossil analysis followed Mauquoy and van Geel (2007), modified by Väliranta *et al* (2007). If plant remains were unidentifiable to plant type level, proportion of unidentified organic matter (UOM) was estimated. Identification followed e.g. Laine *et al* (2009), Mauquoy and van Geel (2007), and Eurola *et al* (1992). A reference collection was also available. Software

C2 (v. 1.7.7) (Juggins 2007) and Tilia 2.0.41 were used to produce the diagrams.

Chronology

Radiocarbon (^{14}C) accelerator mass spectrometry (AMS) and lead (^{210}Pb) dating methods were combined to establish accurate chronologies and build age-depth models (van Der Plicht 2004, Ali *et al* 2008). In total 16 samples were sent to Poznan Radiocarbon Laboratory (Poznan, Poland) and three samples to the Finnish Museum of Natural History (LUOMUS, Helsinki, Finland) for ^{14}C dating (table S1 is available online at stacks.iop.org/ERL/14/075002/mmedia). Bulk peat samples, cleaned of roots and rootlets when possible (Holmquist *et al* 2016), were used for ^{14}C dating. Samples from the base of each peat monolith, layers representing vegetation changes and/or intermediate layers (LG2.2 and K2.3) were selected for dating.

To create accurate chronologies for recent decades, ^{210}Pb dating was performed at the University of Exeter, UK, using alpha-spectrometry. ^{210}Pb was measured at 2 cm intervals for each full-length monolith. Freeze-dried subsamples of 0.14−0.51 g were analysed for ^{210}Pb activity after spiking them with a ^{209}Po yield tracer, following the methods described by Kelly *et al* (2017) and Estop-Aragonés *et al* (2018). ^{210}Pb ages were obtained using the Constant Rate of Supply model (CRS) (Appleby and Oldfield 1978). Age-depth models for each core (figure 2) were created with BACON v2.3.3 package in R version 3.4.3 (R Development Core Team 2016). BACON divides the dated cores into sections and applies Bayesian statistics with prior information to reconstruct the accumulation, providing weighted mean ages (Blaauw 2010, Blaauw and Christen 2011) that are further used for calculations without chronological error ranges. ^{14}C ages were internally calibrated using the INTCAL 13 calibration curve (Reimer 2013) and modern dates (pMC % modern carbon) were converted to radiocarbon ages applying NH Zone 1 post bomb curve (Hua *et al* 2013).

Carbon accumulation rates ACAR and RERCA values

For peat and carbon accumulation calculations, dry bulk density (g cm^{-3}) was measured contiguously for every cm after freeze-drying volumetric subsamples of 5 cm^3 and by dividing the dry mass (g) by the peat fresh volume (cm^3). Carbon and nitrogen (C/N) content measurements were performed at 4 cm intervals, at the University of Helsinki, using a LECO TruSpec micro Elemental Determinator and these results were applied to calculate average carbon values.

To estimate the temporal variations in apparent carbon accumulation rates (ACAR, g C m^{-2} yr^{-1}), the carbon mass of every 1 cm increment (g m^{-3}) was multiplied by the corresponding vertical peat accumulation rate (m yr^{-1}) (Turunen *et al* 2002) based on the age-depth models. Average, non-cumulative, apparent recent rates of carbon accumulation (RERCA) (see Turunen 2003) were calculated for three periods; post AD 1950 until present, post AD 1900 until present, and post AD 1850 until present, following a procedure introduced in Lamarre *et al* (2012). These periods mainly represent incompletely decomposed (acrotelm) peat and are not straight forwardly comparable with results yielded from older highly decomposed, water saturated, and anoxic (catotelm) peat.

Results

Chronology and peat accumulation

Age-depth models show that peat accumulation has not been constant over the accumulation history and ages at the base of the monoliths vary from ca. 2500 cal. BP (K1P2) to ca. cal. AD 1960 (K2.3 and LG2.2) (figure 2). However, in this study, we focus on the period of the last ca. 200 years. Mean peat accumulation rates range from 1.6 to 5.4 mm yr^{-1} (table 2). On average, accumulation rates increase towards the present, starting from the 1950s (figures 3–6). Within both regions, peatland specific variation in accumulation rates exists (table 2). The K1P2 age-depth model suggests a slowdown in peat accumulation between ca. 1800 cal. BP and 95 cal. BP (19–15 cm) when the peat accumulation rate is only 0.02 mm yr^{-1}. Alternatively either of the ^{14}C ages is an outlier. ^{210}Pb activity ceases already at 13 cm below the surface in K1P2 (figure 2). For cores K2.3 and LG2.2 (both 33 cm in length), the ^{210}Pb analyses did not reach the zero activity level (table S2). In order to establish age-depth models for these two cores, we ^{14}C-dated additional peat samples (table S1 and figure 2). Additionally, the ^{14}C basal-age of the record LG2.3 was younger than the corresponding age suggested by the ^{210}Pb chronology (table S2) and the BACON age-depth model therefore excluded the ^{14}C age as an outlier (figure 2). A charcoal layer with charred plant remains in LG2.2 was dated to ca. cal. AD 1940 (21 cm) which corresponds to a previously reported fire in AD 1941 (SOPFEU 2004) and supports the reliability of the chronology (figures 2 and 5).

Peat properties

The average core-specific bulk density (BD) with standard deviation (±SD) varies between 0.05 ± 0.01 g cm^{-3} (LG2.3) and 0.11 ± 0.04 g cm^{-3} (K1P2) with an increasing trend towards older peat layers (figures 3–6). The mean BD of all the cores was 0.07 ± 0.03 g cm^{-3}. Carbon content analysis yielded an average of 45.5% ± 1.7%. Carbon averages calculated over an individual peat core ranged from 43.9% ± 1.4% (K2.3) to 47.1% ± 2.7% (K1P2). C/N ratio varied between 14.3 and 62.8 with an average of 36.4 ± 11.9. The overall trend in C/N values increased towards the surface (figures 3–6).

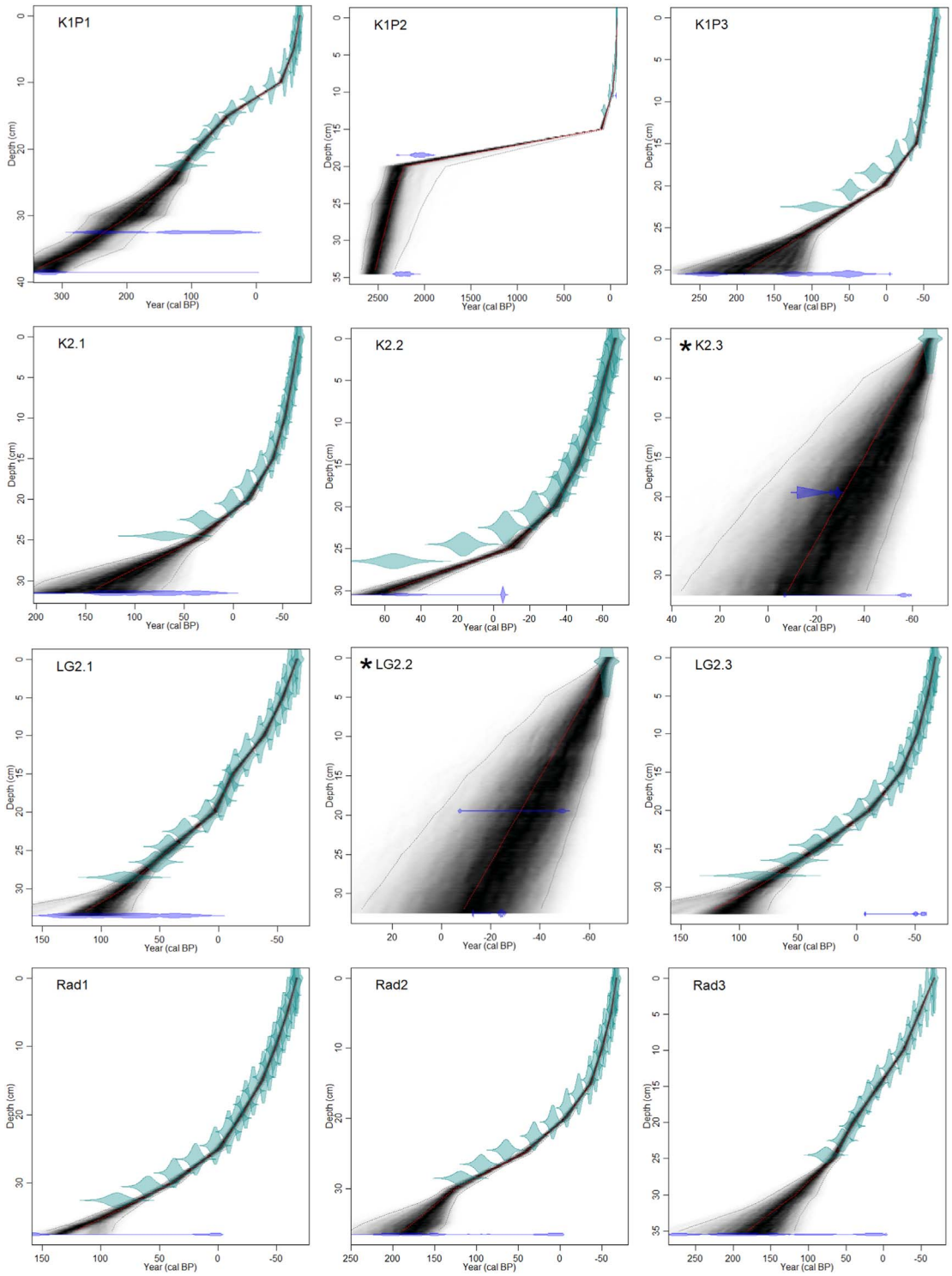

Figure 2. BACON age-depth models. ^{210}Pb age-ranges are in green (for *LG2.2 and *K2.3 green indicates the coring year), and ^{14}C dates (cal. BP) are in blue. The grey shading indicates the possible age-range and darkest grey demarks most likely range. The thin red line in the middle is the weighted mean age based on the model.

Past vegetation succession

Kuujjuarapik (K1P)

At first, until ca. cal. AD 1710 (33 cm), *S. fuscum* dominates in K1P1, after which the dry assemblage is replaced by wet *S. lindbergii* and Cyperaceae (figure S1). Between ca. cal. AD 1960 and cal. AD 2000, at 13–7 cm, the K1P1 record shows a change from a wet assemblage back to a drier assemblage with *Dicranum* sp. and dwarf shrubs. From ca. cal. AD 1990 (9 cm), a *S. fuscum*-ericaceous assemblage dominates.

K1P2 is first dominated by *S. fuscum* with numerous *Picea* sp. needles (33–19 cm), woody material and sparse charred fragments (33–12 cm). Cyperaceous taxa are most abundant between 20 and 11 cm up to ca. cal. AD 1950. Wet *Sphagnum* sect. Cuspidata was identified at 13–11 cm. Shrub roots replace the

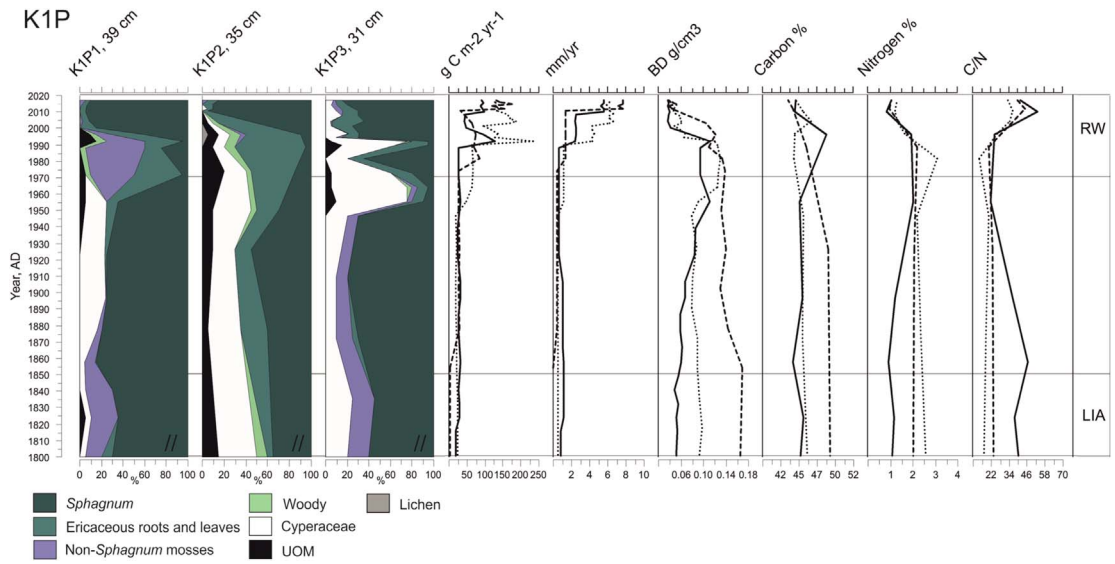

Figure 3. Plant composition presented as main vegetation types with different colours (%). Y-axis indicates the AD year from 1800 until the coring year 2017. Symbol // is used to indicate that the record continues to older ages. Continuous line represents K1P1 record, dashed line K1P2, and dotted line K1P3. On the top x-axis g C m^{-2} yr^{-1} stands for ACAR, mm yr^{-1} for peat accumulation and BD (g cm^{-3}) for bulk density. RW zone (recent warming) and LIA zone (Little Ice Age) are shown with grey horizontal lines.

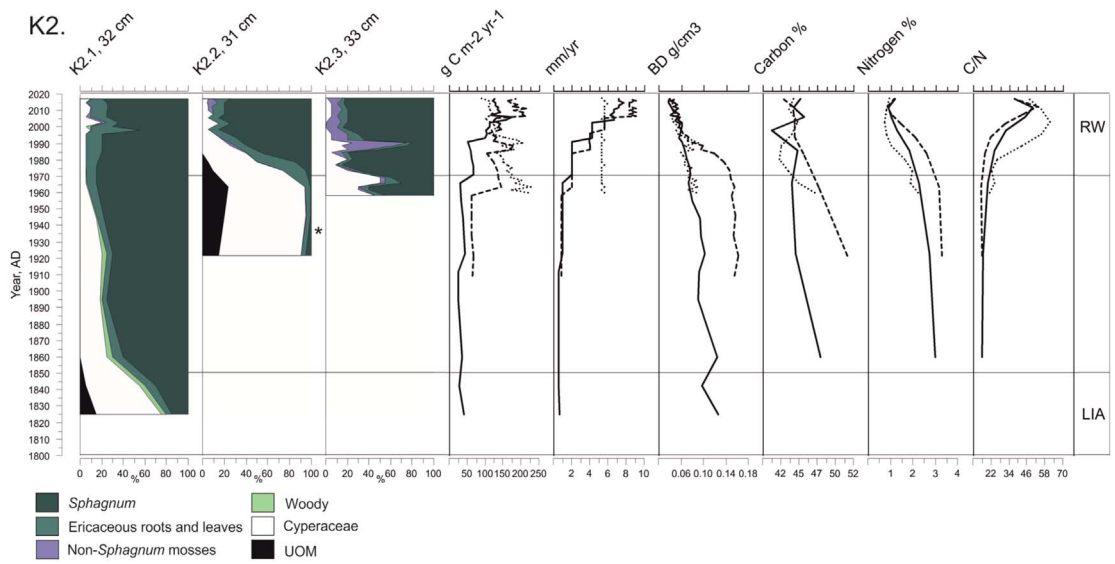

Figure 4. Plant composition presented as main vegetation types with different colours (%). Y-axis indicates the AD year from 1800 until the coring year 2017. Symbol * indicates where charcoal and/or charred plants were found. Continuous line represents K2.1 record, dashed line K2.2, and dotted line K2.3. On the top x-axis g C m^{-2} yr^{-1} stands for ACAR, mm yr^{-1} for peat accumulation and BD (g cm^{-3}) for bulk density. RW zone (recent warming) and LIA zone (Little Ice Age) are shown with grey horizontal lines.

Sphagnum dominance between ca. cal. AD 1950 and 1995 (11–7 cm). *S. fuscum* dominates the vegetation from ca. cal. AD 1995 (7–0 cm) to present.

In K1P3, Cyperaceae and *Sphagnum* assemblages alternate. First (from 31 cm, ca. cal. AD 1765), Cyperaceae spp. dominate until ca. cal. AD 1780 (30–29 cm) when the assemblage shifts to *S. lindbergii*. Non-*Sphagnum* bryophytes e.g. *Straminergon stramineum* and *Exannulata* group species are present through these phases. After ca. cal. AD 1930 (21 cm) *S. lindbergii* is first accompanied by, and then in ca. cal. AD 1970 replaced with Cyperaceae species. *Trichophorum cespitosum* prevails with dwarf shrubs between ca. cal. AD 1970 and ca. cal. AD 1990 (17–15 cm). After ca. cal. AD 1990 (14 cm), *S. russowii* re-establishes the *Sphagnum* assemblage with small quantities of *Trichophorum cespitosum* and ericaceous plants.

Kuujjuarapik (K2)

Cyperaceae spp. dominate the K2.1 record from ca. cal. AD 1825 until ca. cal. AD 1845 (29 cm), when the plant assemblage changes to *Sphagnum fuscum* dominance

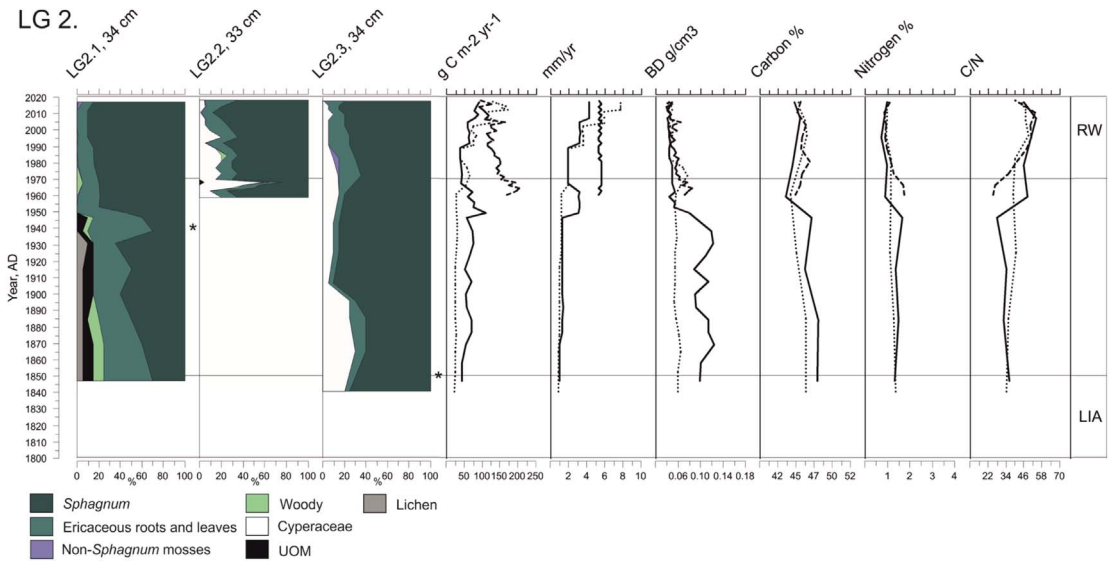

Figure 5. Plant composition presented as main vegetation types with different colours (%). Y-axis indicates the AD year from 1800 until the coring year 2017. Symbol * indicates where charcoal and/or charred plants were found. Continuous line represents LG2.1 record, dashed line LG2.2, and dotted line LG2.3. On the top x-axis g C m^{-2} yr^{-1} stands for ACAR, mm/yr for peat accumulation and BD (g cm^{-3}) for bulk density. RW zone (recent warming) and LIA zone (Little Ice Age) are shown with grey horizontal lines.

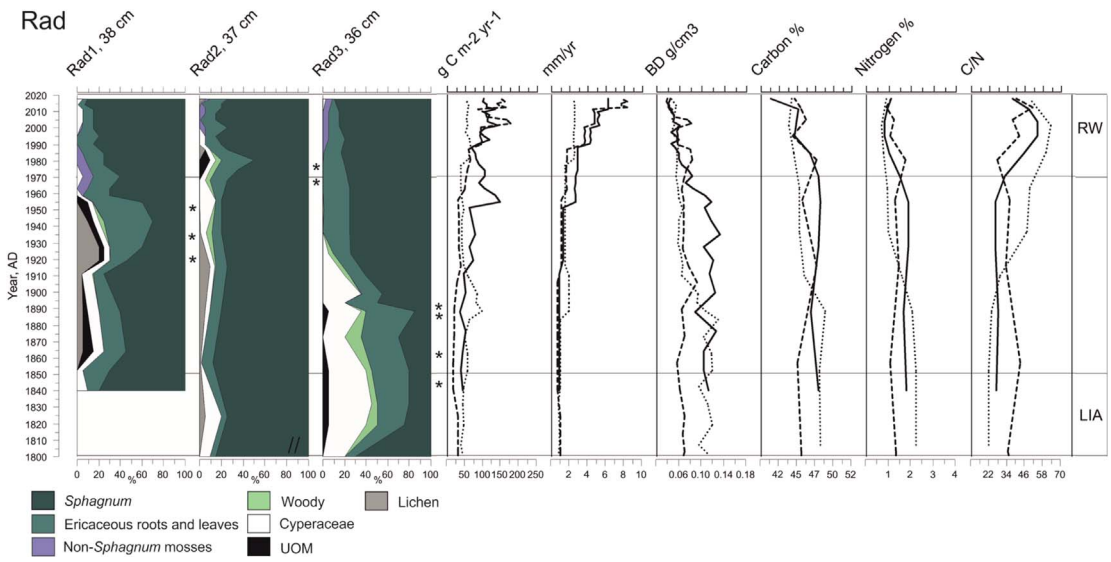

Figure 6. Plant composition presented as main vegetation types with different colours (%). Y-axis indicates the AD year from 1800 until the coring year 2017. Symbol // is used to indicate that the record continues to older ages, and symbol * indicates where charcoal and/or charred plants were found. Continuous line represents Rad1 record, dashed line Rad2, and dotted line Rad3. On the top x-axis g C m^{-2} yr^{-1} stands for ACAR, mm yr^{-1} for peat accumulation and BD (g cm^{-3}) for bulk density. RW zone (recent warming) and LIA zone (Little Ice Age) are shown with grey horizontal lines.

(figure 4). At ca. cal. AD 1995 (13 cm), slightly more Cyperaceae remains, dwarf shrub roots, and Ericaceae leaves (mainly *Chamaedaphne calyculata*) occur.

In K2.2, macroscopic charcoal is detected between ca. cal. AD 1900 (31 cm) and ca. cal. AD 1935 (27 cm). Cyperaceae spp. are present until ca. cal. AD 1980 (21 cm) but are replaced by *S. fuscum* via *S.* sect. *subsecunda* and ericaceous roots. *S. fuscum* dominates the plant assemblages until the present-day together with *Trichophorum cespitosum* and Ericaceae (figures 4, S1).

In K2.3, the assemblages of cyperaceous plants and *S. fuscum* vary between ca. cal. AD 1960 and 1990 (33–16 cm) (figures 4, S1). *Chamaedaphne calyculata* seeds are numerous around cal. AD 1980s (21–18 cm) and *Mylia anomala* is abundant (up to 40%) between ca. cal. AD 1985 and ca. cal. AD 1990 (18–16 cm). From ca. cal. AD 1990 to the present-day, *S. fuscum* dominates the plant assemblages. Dwarf shrub roots, *Trichophorum cespitosum,* and *Polytrichum strictum* occur throughout the record in low quantities.

Radisson (LG2)

The LG2.1 vegetation assemblage is predominantly composed of *Sphagnum capillifolium* together with ligneous plants and some lichens from ca cal. AD 1850 until ca. cal. AD 1945 (20 cm) (figures 5, S1). A layer with charred plant remains occurred ca. cal. AD 1940 (21 cm). After the fire to the present-day, *Sphagnum fuscum* dominates the plant assemblage occasionally accompanied by *Mylia anomala*.

No substantial changes are detected in the LG2.2 plant assemblages. At first, *S. fuscum* is occuring together with cf *S. subfulvum*. After ca. cal. AD 1965, cyperaceous remains become more abundant. *S. fuscum* becomes dominant again after ca. cal. AD 1970 (27 cm), together with some sparse cyperaceous taxa and dwarf shrub roots that prevail throughout the record (figures 5, S1).

In LG2.3, charcoal and charred plant fragments are identified at ca. cal. AD 1850 (31 cm). Until ca. cal. AD 1885 (28 cm), *S. balticum* prevails with *S. fuscum*, *S. rubellum,* and *Trichophorum cespitosum*. After ca. cal. AD 1885, *S. balticum* disappears and *S. fuscum* dominates the plant assemblages with *S. rubellum*, until present. Dwarf shrub roots and *Mylia anomala* are scarce throughout. Ericaceous leaves become more abundant after ca. cal. AD 1965 (19 cm) (figures 5, S1).

Radisson (Rad)

In Rad1 (from 38 cm, ca. cal. AD 1840), *S. fuscum* dominates the assemblage accompanied *by S. rubellum* and *S. capillifolium*. Dwarf shrub roots are abundant (up to 40%) and lichens are found from ca. cal. AD 1920 until ca. cal. AD 1960 (29–23 cm). Charcoal is found between cal. AD 1920s and 1950s (29–25 cm) (figures 6, S1). After the charcoal layers, *S. balticum* and *Mylia anomala* are found and ericaceous plants become more abundant. Towards present, the prevalence of roots declines and *Sphagnum* represents up to 80% of plant remains.

In Rad2 (37 cm: from ca. cal. AD 1770), *S. fuscum* dominates the plant assemblage throughout the record, with a reduction from 75%–90% to 50% after cal. AD 1970s (18–16 cm). Charcoal and charred plant fragments occur between late cal. AD 1960s and mid-1970s (21–17 cm). Some lichens are found underneath the charcoal layer until the cal. AD 1930s (23 cm) and at 16 cm which corresponds to the late cal. AD 1980s. Cyperaceous taxa are found in small abundance until ca. cal. AD 1990 (13 cm). In the plant assemblages following the charcoal layers, *Mylia anomala* appears with ericaceous shrubs up to the present-day surface.

From the base of Rad3 record (36 cm, ca. cal. AD 1780), until ca. cal. AD 1820 (32 cm), cf *S. subfulvum* is abundant together with Cyperaceae species. Charcoal and charred plant fragments are detected between ca. cal. AD 1820–1890 (32–24 cm). After ca. cal. AD 1820, *Sphagnum* remains diminish with an increase in dwarf shrub roots. *Sphagnum* sect. Cuspidata occurs until ca. cal. AD 1880 (25 cm), when replaced by *S. fuscum* and *S. rubellum*. *Picea mariana* needles are numerous around ca. cal. AD 1880s (25 cm). After the last charcoal layer (ca. cal. AD 1890), *S. rubellum* and *S. fuscum* accompanied by dwarf shrub roots dominate the record (figures 6, S1).

ACAR and RERCA variability

Because the ages at the base of the monoliths vary, the oldest dated to 2510 cal. BP (K1P2) and youngest to −10 cal. BP (cal. AD 1960, K2.3 and LG2.2), we focused on three defined RERCA periods: from AD 1850, from AD 1900, and from AD 1950 to the present-day (table 2). This approach enables us to identify and compare possible changes in recent carbon accumulation rates. In general, the post AD 1950 RERCA rates are the highest (table 2, figures 3–6), partly due to incomplete decomposition. At K2, RERCA values were consistently high (table 2). The lowest post AD 1950 RERCA rates were detected for the Radisson region peatlands: LG2.1: 65.3 g C m^{-2} yr^{-1} and Rad3: 50.7 g C m^{-2} yr^{-1}. However, for these same peatlands, much higher rates were also derived: LG2.2: 136.9 g C m^{-2} yr^{-1} and Rad1: 103.3 g C m^{-2} yr^{-1}.

ACAR variability is high (figure 7) and mainly varies with depth, with higher rates towards the peat surfaces (figures 3–6). RERCA ranges and exact values for the three focus periods are higher for Kuujjuarapik than for Radisson peatlands (e.g. AD 1950 RERCAs are 24% higher in Kuujjuarapik region than in Radisson) (figure 7). The site-combined averages for the three periods were consistently higher in Kuujjuarapik than in Radisson, but also the lowest apparent carbon accumulation rates were calculated for Kuujjuarapik (figure 7).

Discussion

Variations in vegetation succession patterns between and within sites neither fully support nor reject our first research question that plant assemblages are changing synchronously in response to rapid recent warming. In contrast to our second research question, the northern Kuujjarapik peatlands had higher RERCA rates when compared to the more southern Radisson site but supporting the research question, carbon accumulation rates increased towards recent decades. This increase is, however, partly expected due to the incomplete state of decomposition even if the climate had not become warmer. Plant assemblages of K2, Rad, and LG2 peatlands revealed asynchronous response to post-LIA warming (figures 4–6). Moreover, all sampling sites indicated more recent decadal-scale changes; yet the exact timing varies (figures 3–6). In K1P peatland, the vegetation change was synchronous for all records starting from ca. cal. AD 1950s and lasting until mid-1990s resulting with an establishment of a drier *Sphagnum* lawn microform. In turn, at K2 peatland, the vegetation assemblages showed

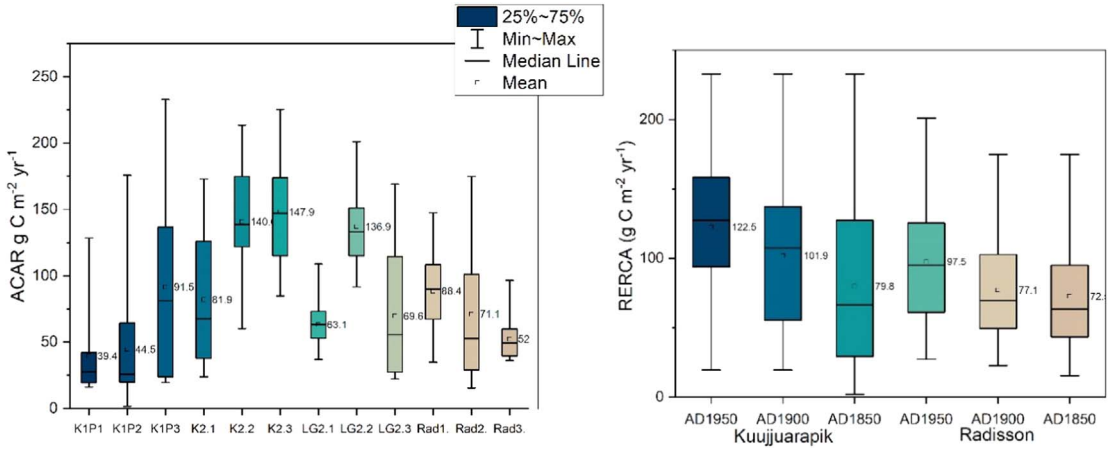

Figure 7. ACAR (g C m^{-2} yr^{-1}) variability for each core (left panel) and combined RERCA (g C m^{-2} yr^{-1}) variability for the two study regions, Kuujjuarapik and Radisson, focusing on three periods: from AD 1950, from AD 1900, and from AD 1850 to present (right panel). See legend in the left panel.

successional changes around cal. AD 1970s (K2.2), 1980s (K2.3), and 1990s (K2.1). However, K2 peatland has different permafrost dynamics and microtopography gradient from K1P palsa peatland. Vegetation community changes in Rad peatland and the LG2.1 record around cal. AD 1940s might have been fire-induced as suggested by the charred plant remains and charcoal in the peat records. Kuujjuarapik vegetation assemblages seem to have experienced more synchronous and distinct changes than the southern, Radisson assemblages. This could be linked to changes in thawing permafrost dynamics in the northern Kuujjuarapik site.

Peat properties and peat and carbon accumulation

Our BD values corresponded to previous studies from Northern Ontario where BD ranged from 0.0034 to 0.62 g cm^{-3} with an average of 0.093 $\pm$ 0.041 g cm^{-3} (Holmquist *et al* 2014). Our average carbon content was slightly lower than the 50% which is often used for peat carbon content calculations for boreal and subarctic to Arctic regions (Turunen *et al* 2002, Treat *et al* 2016), but close to an average reported for northern peatlands 46.8% $\pm$ 6.1% (Loisel *et al* 2014). Our C/N averages are comparable with other studies, but our lowest C/N values were lower than those reported by Treat *et al* (2016) (C/N 30–62).

Previous results from Kuujjuarapik have shown a notable rise of peat accumulation rates since the beginning of the 20th century, with average RERCAs: 133–147 g C m^{-2} yr^{-1} from cal. AD 1950 to present, 73–81 g C m^{-2} yr^{-1} from cal. AD 1900 to present, and 52–62 g C m^{-2} yr^{-1} from cal. AD 1850 to present (Lamarre *et al* 2012). The highest individual RERCA values of Lamarre *et al* (2012) exceeded 160 g C m^{-2} yr^{-1} and were interpreted to reflect the recent increase in annual temperatures.

High peat accumulation rates of 0.5 cm yr^{-1}, with an average of 0.037 cm yr^{-1}, and high RERCA values (form cal. AD 1850) between 52.8 and 114.5 g C m^{-2} yr^{-1} with a mean of 73.6 g C m^{-2} yr^{-1}, have been reported for Eastmain, James Bay area south from Radisson (Loisel and Garneau 2010). Moreover, a mean carbon accumulation rate over the past ca. 300 years of 56.4 g C m^{-2} yr^{-1}, has been obtained from the same region (van Bellen *et al* 2011b). Turunen *et al* (2004) reported a carbon accumulation rate of 73 g C m^{-2} yr^{-1} for eastern Canadian bogs, covering the last 150 years. High carbon accumulation rates of $>$ 150 g C m^{-2} yr^{-1} over the past ca. 200 years in northeastern maritime Québec have been put forward by Magnan and Garneau (2014a). In contrast, Hudson Bay Lowland records from Northern Ontario indicated no rise in carbon accumulation rates for the recent decades, i.e. less than 30 g C m^{-2} yr^{-1} (Bunbury *et al* 2012). There, the lead activity covered only the topmost 6 cm, while in the current study, where the core lengths were between 31 cm and 39 cm, the zero ^{210}Pb activity level was sometimes not reached at all (K2.3 and LG2.2), which creates uncertainty for the chronologies. However, in K1P2, the lead activity covered only the topmost 13 cm, resembling the results of Bunbury *et al* (2012). These previous studies were conducted in peatlands resembling ours and samples were mainly collected from similar microhabitats. It has been suggested that peat and carbon accumulation rates are fast for *Sphagnum*-dominated habitats under high effective moisture conditions and slower when sedges dominate in warm and dry conditions (Nichols *et al* 2014). In the La Grande region, a rise in peat accumulation rates together with a recent change towards *Sphagnum*-dominated plant communities has been detected (Beaulieu-Audy *et al* 2009, Pratte *et al* 2017). In our study, however, we found no correlation between *Sphagnum* assemblages and carbon accumulation (Pearson correlation: $r = 0.09$, $p = 0.21$).

Drivers behind accumulation patterns

Intermediate peatland microforms, selected for this study, have higher vertical peat and carbon accumulation rates than, for instance, wet hollows or high and dry hummocks (Belyea and Clymo 2001). *Sphagnum* establishment promotes rapid peat accumulation and hence peatland vegetation community structure strongly influences carbon sequestration (Tuittila *et al* 2012, Loisel and Yu 2013). However, it is often a challenge to separate internal and site-specific and external, e.g. climate driven, forcing (Loisel and Garneau 2010, van Bellen *et al* 2011b, Tuittila *et al* 2007, 2012, Loisel and Yu 2013). Changes in hydrology and vegetation can also be caused by long-term hydroseral succession from fen to bog (ombrotrophication) that is driven by both internal and external forcing (Yu *et al* 2009, Väliranta *et al* 2017).

PAR0 and growing season length have been connected to *Sphagnum* productivity (NPP) (Loisel *et al* 2012, Gallego-Sala *et al* 2018). Accordingly, peat accumulation should be positively correlated to GDD0 (Clymo *et al* 1998, Charman *et al* 2013, Holmquist *et al* 2014). In addition, moisture is an important factor controlling carbon accumulation and peatland dynamics (Swindles *et al* 2015, Gałka *et al* 2017, Zhang *et al* 2018a). Both precipitation and GDD0 have increased since the 1960s and 1970s in our study sites (Environment Canada 2018). In the Hudson Bay region, sea ice cover has decreased up to 11.3% $\pm$ 2.6% per decade from AD 1971 to AD 2008, which is affecting moisture and heat transfer patterns of the area (Tivy *et al* 2011) and may also affect peat accumulation processes.

Our aim was to study recent peat and carbon accumulation patterns by collecting peat records from uniform lawn *Sphagnum* microforms. Because establishment of robust chronologies for young peat sections is challenging (see however e.g. Goslar *et al* 2005), in this study we combined two dating methods that support each other (e.g. Turetsky *et al* 2004). Our results indicated high accumulation rates during recent decades. Previous studies focussing on both the last millennium (Charman *et al* 2013, Garneau *et al* 2014, Loisel *et al* 2014) and recent decades (Zhang *et al* 2018b) showed that relatively high accumulation rates are likely caused by increased carbon inputs rather than by reduced decomposition. We acknowledge the difficulty of interpreting the recent peat accumulation rates due to the incomplete decomposition process and lower compaction of the surface peat and restraints on the chronologies. Despite these inaccuracies, by using specified focus periods, the data nevertheless allow spatio-temporal comparisons and the assessment of data against the previously published data carried out using similar protocols.

Future implications

Observed and anticipated warmer and wetter climate conditions for the coming decades (Kirtman *et al* 2013, Environment Canada 2018) should be beneficial for peat accumulation (Payette *et al* 2004). Following this, a potential increase of carbon storage has been suggested (Holmquist *et al* 2014, Gallego-Sala *et al* 2018). However, contrasting views also exist where modelling exercises suggest that in eastern Canada, peatlands will turn into a carbon source due to increased decomposition under warmer climate, despite the potential increase in carbon sequestration (Chaudhary *et al* 2017). McGuire *et al* (2018) modelled the vegetation response to climate warming and CO_2 fertilization under different warming scenarios. They predicted that depending on the magnitude of warming, northern permafrost soils could act as a net sink of carbon, but if the warming is more prominent, substantial soil carbon losses could appear after 2100 (McGuire *et al* 2018). In some of the projections, vegetation was largely responsible for the carbon intake, but the other projections indicated that vegetation carbon intake could not compensate the losses (McGuire *et al* 2018). To address the question how high-latitude peatland vegetation and carbon dynamics will respond and have responded to recent warming, more data are needed including high-resolution chronologies and multiple cores, as presented in this study. The presented data highlight the importance of studying multiple peat sections from one study site and preferably the approach should be extended to regional-scales as stated by our third research question and the internal variability needs to be take into account when thinking about upscaling and modelling of results (Loisel and Garneau 2010, Lamarre *et al* 2012, Mathijssen *et al* 2017, Zhang *et al* 2018a).

Conclusions

This study analysed twelve shallow surface peat cores for plant macrofossils and carbon accumulation to reveal recent changes in habitat conditions and peat properties in northern peatlands of eastern Canada. Our results indicated more prominent changes in vegetation dynamics and carbon accumulation in the northernmost study sites than in the southern sites. These changes may be linked to larger increase in the growing season length, different climatic conditions, and changing permafrost dynamics of the northern region. High-resolution chronologies, by applying multiple complimentary dating methods, is essential to reveal the most recent changes. Our study shows that in order to exclude the influence of internal peatland variability on detected changes in accumulation patterns, multiple cores are needed to capture the genuine regional-scale climate signal.

Acknowledgments

We thank N Chaumont for fieldwork assistance, N Sanderson for helping with establishing the chronologies,

and R Gauthier for rechecking one *Sphagnum* species. The Academy of Finland (code 296519) and Natural Sciences and Engineering Research Council of Canada (NSERC; No. 250287) discovery grant to MG funded this project. We thank the three anonymous reviewers for their constructive comments.

ORCID iDs

Sanna R Piilo https://orcid.org/0000-0002-9054-1542
Minna M Väliranta https://orcid.org/0000-0003-0129-7240

References

Abram N J *et al* the PAGES 2k Consortium 2016 Early onset of industrial-era warming across the oceans and continents *Nature* **536** 411–8
Ali A A *et al* 2008 Recent peat accumulation rates in minerotrophic peatlands of the Bay James region, Eastern Canada, inferred by 210Pb and137Cs radiometric techniques *Appl. Radiat. Isot.* **66** 1350–8
Allard M and K-Seguin M 1987 Le pergélisol au Québec nordique: bilan et perspectives *Géogr. Phys. Quaternaire* **41** 141–52
Appleby P G and Oldfield F 1978 The calculation of lead-210 dates assuming a constant rate of supply of unsupported 21 ° Pb to the sediment *Catena* **5** 1–8
Arlen-Pouliot Y and Bhiry N 2005 Palaeoecology of a palsa and a filled thermokarst pond in a permafrost peatland, subarctic Québec, Canada *Holocene* **15** 408–19
Arseneault D and Sirois L 2004 The millennial dynamics of a boreal forest stand from *J. Ecol.* **92** 490–504
Beaulieu-Audy V *et al* 2009 Holocene palaeoecological reconstruction of three boreal peatlands in the la Grande Rivire region, Qu©bec, Canada *Holocene* **19** 459–76
Belyea L R and Clymo R S 2001 Feedback control of the rate of peat formation *Proc. R. Soc.* B **268** 1315–21
Blaauw M 2010 Methods and code for 'classical' age-modelling of radiocarbon sequences *Quat. Geochronol.* **5** 512–8
Blaauw M and Christen J A 2011 Flexible paleoclimate age-depth models using an autoregressive gamma process *Bayesian Anal.* **6** 457–74 (https://projecteuclid.org/euclid.ba/1339616472)
Bunbury J, Finkelstein S A and Bollmann J 2012 Holocene hydro-climatic change and effects on carbon accumulation inferred from a peat bog in the Attawapiskat River watershed, Hudson Bay Lowlands, Canada *Quat. Res.* **78** 275–84
Carroll P and Crill P 1997 Carbon balance of a temperate poor fen *Glob. Biogeochem. Cycles* **11** 349–56
Charman D J, Aravena R and Warnert B G 1994 Carbon Dynamics in a Forested Peatland in North-Eastern Ontario, Canada *J. Ecol.* **82** 55–62
Charman D J *et al* 2013 Climate-related changes in peatland carbon accumulation during the last millennium *Biogeosciences* **10** 929–44
Charman D J *et al* 2015 Drivers of Holocene peatland carbon accumulation across a climate gradient in northeastern North America *Quat. Sci. Rev.* **121** 110–9
Chaudhary N, Miller P A and Smith B 2017 Modelling past, present and future peatland carbon accumulation across the pan-Arctic region *Biogeosciences* **14** 4023–44
Clymo R S, Turunen J and Tolonen K 1998 Carbon Accumulation in Peatland *Oikos* **81** 368–388 (http://www.jstor.org/stable/3547057)
Collins M *et al* 2013 Long-term climate change: projections, commitments and irreversibility *Climate Change 2013: The Physical Science Basis. Contribution of Working Group I to the Fifth Assessment Report of the Intergovernmental Panel on Climate Change* ed T F Stocker *et al* (Cambridge: Cambridge University Press) pp 1029–136
Crowther T W *et al* 2016 Quantifying global soil carbon losses in response to warming *Nature* **540** 104–8
Davidson E A and Janssens I A 2006 Temperature sensitivity of soil carbon decomposition and feedbacks to climate change *Nature* **440** 165–73
Dorrepaal E *et al* 2009 Carbon respiration from subsurface peat accelerated by climate warming in the subarctic *Nature* **460** 616–9
Dyke A S and Prest V K 1987 Late Wisconsinan and Holocene history of the laurentide ice sheet *Géogr. Phys. Quaternaire* **41** 237–63
Environment Canada 2018 Canadian climate normals – climate – environment and climate change Canada (http://climate.weather.gc.ca/climate_normals/) (Accessed: 28 February 2018)
Estop-Aragonés C *et al* 2018 Limited release of previously-frozen C and increased new peat formation after thaw in permafrost peatlands *Soil Biol. Biochem.* **118** 115–29
Eurola S, Bendiksen K and Rönkä A 1992 Suokasviopas. 2. korjattu painos *Oulanka Reports* ed J Viramo (Oulanka Biological Station, University of Oulu, Finland) p 205
Frolking S and Roulet N T 2007 Holocene radiative forcing impact of northern peatland carbon accumulation and methane emissions *Glob. Change Biol.* **13** 1079–88
Frolking S, Talbot J and Subin Z M 2014 Exploring the relationship between peatland net carbon balance and apparent carbon accumulation rate at century to millennial time scales *Holocene* **24** 1167–73
Gallego-Sala A V *et al* 2018 Latitudinal limits to the predicted increase of the peatland carbon sink with warming *Nat. Clim. Change* **8** 907–13
Garneau M *et al* 2014 Holocene carbon dynamics of boreal and subarctic peatlands from Québec, Canada *Holocene* **24** 1043–53
Gałka M *et al* 2017 Vegetation succession, carbon accumulation and hydrological change in Subarctic Peatlands, Abisko, Northern Sweden *Permafrost Periglacial Process.* **28** 589–604
Gałka M *et al* 2018 Response of plant communities to climate change during the late Holocene: palaeoecological insights from peatlands in the Alaskan Arctic *Ecol. Indicators* **85** 525–36
Gorham E 1991 Northern peatlands: role in the carbon cycle and probable responses to climatic warming *Ecol. Appl.* **1** 182–95
Goslar T *et al* 2005 Radiocarbon dating of modern peat profiles: pre- and post-bomb 14C variations in the construction of age-depth models *Radiocarbon* **47** 115–34
Holmquist J R *et al* 2016 A comparison of radiocarbon ages derived from bulk peat and selected plant macrofossils in basal peat cores from circum-arctic peatlands *Quat. Geochronol.* **31** 53–61
Holmquist J R, MacDonald G M and Gallego-Sala A 2014 Peatland initiation, carbon accumulation, and 2 ka depth in the James bay lowland and adjacent regions *Arctic, Antarct., Alpine Res.* **46** 19–39
Hua Q, Barbetti M and Rakowski A Z 2013 Atmospheric radiocarbon for the period 1950–2010 *Radiocarbon* **55** 2059–72
IPCC 2013 Summary for policymakers *Climate Change 2013: The Physical Science Basis. Contribution of Working Group I to the Fifth Assessment Report of the Intergovernmental Panel on Climate Change* (Cambridge: Cambridge University Press) p 33
Ise T *et al* 2008 High sensitivity of peat decomposition to climate change through water-table feedback *Nat. Geosci.* **1** 763–6
Jean M and Payette S 2014 Effect of vegetation cover on the ground thermal regime of wooded and non-wooded palsas *Permafrost Periglacial Process.* **25** 281–94
Juggins S 2007 *C2 User Guide: Software for Ecological and Palaeoecological Data Analysis and Visualization* (Newcastle

upon Tyne: University of Newcastle) pp 1–73 http://scholar.google.com/scholar?hl=en&btnG=Search&q=intitle:C2+Software+for+ecological+and+palaeoecological+data+analysis+and+visualisation#0

Kelly T J *et al* 2017 The vegetation history of an Amazonian domed peatland *Palaeogeogr. Palaeoclimatol. Palaeoecol.* **468** 129–41

Kirtman B *et al* 2013 Near-term climate change: projections and predictability *Climate Change 2013—The Physical Science Basis* ed T F Stocker *et al* (Cambridge: Cambridge University Press) pp 953–1028

Laine J, Harju P, Timonen T, Laine A, Tuittila E-S, Minkkinen K and Vasander H 2009 *The Intricate Beauty of Sphagnum Mosses—A Finnish Guide to Identification* (Helsinki: University of Helsinki Department of Forest Ecology, Publications) p 39

Lamarre A, Garneau M and Asnong H 2012 Holocene paleohydrological reconstruction and carbon accumulation of a permafrost peatland using testate amoeba and macrofossil analyses, Kuujjuarapik, subarctic Qu??bec, Canada *Rev. Palaeobotany Palynol.* **186** 131–41

Loisel J *et al* 2014 A database and synthesis of northern peatland soil properties and Holocene carbon and nitrogen accumulation *Holocene* **24** 1028–42

Loisel J, Gallego-Sala A V and Yu Z 2012 Global-scale pattern of peatland Sphagnum growth driven by photosynthetically active radiation and growing season length *Biogeosciences* **9** 2737–46

Loisel J and Garneau M 2010 Late Holocene paleoecohydrology and carbon accumulation estimates from two boreal peat bogs in eastern Canada: potential and limits of multi-proxy archives *Palaeogeogr. Palaeoclimatol. Palaeoecol.* **291** 493–533

Loisel J and Yu Z 2013 Surface vegetation patterning controls carbon accumulation in peatlands *Geophys. Res. Lett.* **40** 5508–13

Magnan G *et al* 2018 Impact of the Little Ice Age cooling and 20th century climate change on peatland vegetation dynamics in central and northern Alberta using a multi-proxy approach and high-resolution peat chronologies *Quat. Sci. Rev.* **185** 230–43

Magnan G and Garneau M 2014a Climatic and autogenic control on Holocene carbon sequestration in ombrotrophic peatlands of maritime Quebec, eastern Canada *Holocene* **24** 1054–62

Magnan G and Garneau M 2014b Evaluating long-term regional climate variability in the maritime region of the St. Lawrence North Shore (eastern Canada) using a multi-site comparison of peat-based paleohydrological records *J. Quat. Sci.* **29** 209–20

Mathijssen P J H *et al* 2016 Reconstruction of Holocene carbon dynamics in a large boreal peatland complex, southern Finland *Quat. Sci. Rev.* **142** 1–15

Mathijssen P J H *et al* 2017 Lateral expansion and carbon exchange of a boreal peatland in Finland resulting in 7000 years of positive radiative forcing *J. Geophys. Res.: Biogeosci.* **122** 562–77

Mauquoy D and van Geel B 2007 Plant macrofossil methods and studies: mire and peat macros *Encyclopedia of Quaternary Science* ed S A Elias (Amsterdam: Elsevier) pp 2315–36

McGuire A D *et al* 2009 Sensitivity of the carbon cycle in the Arctic to climate change *Ecol. Monogr.* **79** 523–55

McGuire A D *et al* 2018 Dependence of the evolution of carbon dynamics in the northern permafrost region on the trajectory of climate change *Proc. Natl Acad. Sci.* **15** 3882–7

Naulier M *et al* 2015 A millennial summer temperature reconstruction for northeastern Canada using oxygen isotopes in subfossil trees *Clim. Past* **11** 1153–64

Nichols J E *et al* 2014 Impacts of climate and vegetation change on carbon accumulation in a south-central Alaskan peatland assessed with novel organic geochemical techniques *Holocene* **24** 1146–55

Ovenden L 1990 Peat accumulation in northern wetlands *Quat. Res.* **33** 377–86

Packalen M S and Finkelstein S A 2014 Quantifying Holocene variability in carbon uptake and release since peat initiation in the Hudson Bay Lowlands, Canada *Holocene* **24** 1063–74

Packalen M S, Finkelstein S A and McLaughlin J W 2014 Carbon storage and potential methane production in the Hudson Bay Lowlands since mid-Holocene peat initiation *Nat. Commun.* **5** 4078

PAGES 2k Consortium 2013 Continental-scale temperature variability during the past two millennia *Nat. Geosci.* **6** 339–46

Payette S *et al* 2004 Accelerated thawing of subarctic peatland permafrost over the last 50 years *Geophys. Res. Lett.* **31** 1–4

Pratte S, Garneau M and De Vleeschouwer F 2017 Increased atmospheric dust deposition during the Neoglacial in a boreal peat bog from north-eastern Canada *Palaeogeogr. Palaeoclimatol. Palaeoecol.* **469** 34–46

R Development Core Team 2016 R: A language and environment for statistical com- puting (Vienna: R Foundation for Statistical Computing)

Reimer P 2013 IntCal13 and marine13 radiocarbon age calibration curves 0–50,000 Years cal BP *Radiocarbon* **55** 1869–87

SOPFEU (Société de protection contre les feux) 2004 *Mapping and Dating of Fires in Bay James Area, 1976–2004* (Québec: Radisson/Val-d'Or office)

Swindles G T *et al* 2012 Ecohydrological feedbacks confound peat-based climate reconstructions *Geophys. Res. Lett.* **39** 2–5

Swindles G T *et al* 2015 The long-term fate of permafrost peatlands under rapid climate warming *Sci. Rep.* **5** 17951

Thibault S and Payette S 2009 Recent permafrost degradation in bogs of the james bay area, Northern Quebec, Canada *Permafrost Periglacial Process.* **20** 383–9

Tivy A *et al* 2011 Trends and variability in summer sea ice cover in the Canadian arctic based on the Canadian ice service digital archive, 1960–2008 and 1968–2008 *J. Geophys. Res.: Oceans* **116** C03007

Treat C C *et al* 2016 Effects of permafrost aggradation on peat properties as determined from a pan-Arctic synthesis of plant macrofossils *J. Geophys. Res.: Biogeosci.* **121** 78–94

Tuittila E-S *et al* 2007 Quantifying patterns and controls of mire vegetation succession in a southern boreal bog in Finland using partial ordinations *J. Vegetation Sci.* **18** 891–902

Tuittila E S *et al* 2012 Wetland chronosequence as a model of peatland development: Vegetation succession, peat and carbon accumulation *Holocene* **23** 25–35

Turetsky M, Manning S and Wieder R 2004 Dating recent peat deposits *Wetlands* **24** 324–56

Turunen J *et al* 2002 Estimating carbon accumulation rates of undrained mires in Finland–application to boreal and subarctic regions *Holocene* **12** 69–80

Turunen J 2003 Past and present carbon accumulation in undisturbed boreal and subarctic mires: a review *Suo* **54** 15–28

Turunen J *et al* 2004 Nitrogen deposition and increased carbon accumulation in ombrotrophic peatlands in eastern Canada *Glob. Biogeochem. Cycles* **18** 1–12

Väliranta M *et al* 2007 High-resolution reconstruction of wetness dynamics in a southern boreal raised bog, Finland, during the late Holocene: a quantitative approach *Holocene* **17** 1093–107

van Bellen S *et al* 2011b Quantifying spatial and temporal Holocene carbon accumulation in ombrotrophic peatlands of the Eastmain region, Quebec, Canada *Glob. Biogeochem. Cycles* **25** 1–15

van Bellen S, Garneau M and Booth R K 2011a Holocene carbon accumulation rates from three ombrotrophic peatlands in boreal Quebec, Canada: Impact of climate-driven ecohydrological change *Holocene* **21** 1217–31

van Der Plicht J 2004 Radiocarbon calibration—past, present and future *Nucl. Instrum. Methods Phys. Res.* B **223–224** 353–8

Väliranta M *et al* 2017 Holocene fen–bog transitions, current status in Finland and future perspectives *Holocene* **27** 752–64

Wilson R *et al* 2016 Last millennium northern hemisphere summer temperatures from tree rings: part I: the long term context *Quat. Sci. Rev.* **134** 1–18

Yu Z *et al* 2010 Global peatland dynamics since the last glacial maximum *Geophys. Res. Lett.* **37** 1–5

Yu Z 2011 Holocene carbon flux histories of the world's peatlands: global carbon-cycle implications *Holocene* **21** 761–74
Yu Z, Beilman D W and Jones M C 2009 Sensitivity of Northern Peatland carbon dynamics to Holocene climate change *Carbon Cycling in Northern Peatlands (Geophysical Monograph Series vol 184)* ed A Baird *et al* (Washington, DC: AGU) pp 55–69
Zhang H *et al* 2018a The role of climate change in regulating Arctic permafrost peatland hydrological and vegetation change over the last millennium *Quat. Sci. Rev.* **182** 121–30
Zhang H *et al* 2018b Inconsistent response of Arctic permafrost peatland carbon accumulation to warm climate phases *Glob. Biogeochem. Cycles* **32** 1605–20